Charge dynamics at heterojunctions for PbS/ZnO colloidal quantum dot solar cells probed with time-resolved surface photovoltage spectroscopy

Cite as: Appl. Phys. Lett. **108**, 091603 (2016); https://doi.org/10.1063/1.4943077
Submitted: 05 October 2015 . Accepted: 18 February 2016 . Published Online: 01 March 2016

B. F. Spencer, M. A. Leontiadou, P. C. J. Clark, A. I. Williamson, M. G. Silly, F. Sirotti, S. M. Fairclough, S. C. E. Tsang, D. C. J. Neo, H. E. Assender, A. A. R. Watt, and W. R. Flavell

Charge dynamics at heterojunctions for PbS/ZnO colloidal quantum dot solar cells probed with time-resolved surface photovoltage spectroscopy

B. F. Spencer,[1,a)] M. A. Leontiadou,[1] P. C. J. Clark,[1] A. I. Williamson,[1] M. G. Silly,[2] F. Sirotti,[2] S. M. Fairclough,[3,b)] S. C. E. Tsang,[3] D. C. J. Neo,[4] H. E. Assender,[4] A. A. R. Watt,[4] and W. R. Flavell[1]

[1]*School of Physics and Astronomy and the Photon Science Institute, The University of Manchester, Manchester M13 9PL, United Kingdom*
[2]*Synchrotron SOLEIL, BP 48, Saint-Aubin, F91192 Gif-sur-Yvette Cedex, France*
[3]*Department of Chemistry, University of Oxford, South Parks Road, Oxford OX1 3QR, United Kingdom*
[4]*Department of Materials, University of Oxford, Parks Road, Oxford OX1 3PH, United Kingdom*

(Received 5 October 2015; accepted 18 February 2016; published online 1 March 2016)

Time-resolved laser-pump X-ray-photoemission-probe spectroscopy of a ZnO $(10\bar{1}0)$ substrate with and without PbS quantum dots (QDs) chemically linked to the surface is performed, using laser photon energies resonant with and below the band gap energy of the substrate ($\lambda = 372$ and 640 nm, $h\nu = 3.33$ and 1.94 eV). Charge injection from the photoexcited QDs to ZnO is demonstrated through the change in the surface photovoltage of the ZnO substrate observed when the heterojunction is illuminated with 1.94 eV radiation. The measured carrier dynamics are limited by the persistent photoconductivity of ZnO, giving dark carrier lifetimes of the order of 200 μs in a depletion layer at the interface. The chemical specificity of soft X-rays is used to separately measure the charge dynamics in the quantum dots and the substrate, yielding evidence that the depletion region at the interface extends into the PbS QD layer.
[http://dx.doi.org/10.1063/1.4943077]

Understanding the charge carrier dynamics within nanoscale materials is essential for optimal integration into next-generation technologies. Colloidal quantum dot (QD) solar energy technologies (where the QDs harvest the light, with ZnO or another semiconductor oxide as photoanode)[1] offer the opportunity to engineer the QD effective band gap to maximize solar spectrum absorption, and the possibility of large reductions in the cost-per-watt of solar energy.[2] Research into lead chalcogenide-oxide heterojunctions, where the materials involved are highly abundant on Earth, has increased rapidly, and the optimization of device architectures has developed in several areas that all impact upon device efficiency: passivation of QD surface traps to extend recombination times;[3] ligand exchange to reduce inter-particle spacing and enhance carrier mobility;[4] QD size optimization to engineer the band alignment of QDs to an oxide;[5,6] and carrier multiplication effects for short wavelength photons.[7] The creation of a new device architecture, the depleted heterojunction colloidal quantum dot solar cell (which relies on an interface depletion layer for field-driven charge transport and separation)[8] has had a marked impact, and certified power conversion efficiencies more than 9% have been demonstrated recently.[9,10] The *n*-type substrate induces a depletion region in the *p*-type QD layer,[11] often extending 100–200 nm,[12,13] and it has been shown that device efficiencies increase with layer thickness up to the depletion width.[12,13] Most of these studies have involved measuring the extrinsic properties of heterojunction devices. In this letter, we report on the intrinsic carrier dynamics within a model system of PbS QDs chemically linked to the ZnO $(10\bar{1}0)$ surface, measured using time-resolved photoemission of both the substrate and QDs. This enables us to measure carrier dynamics within a few nm of the interface in a chemically resolved way by probing the electronic environment of atoms on both sides of the interface. Using radiation with energy below the band gap of ZnO, we demonstrate injection of photocarriers from the QDs into ZnO and show that the QDs lie within the depletion field at the interface.

Time-resolved laser-pump photoemission-probe spectroscopy is an ideal probe of carrier dynamics within depletion regions.[14] When carriers are injected into a depletion region at an interface, the band bending across the space charge layer is reduced, and this surface photovoltage (SPV) can be monitored by measuring changes in core-level photoelectron binding energies (BEs). Fast X-ray photoelectron spectroscopy (XPS) then allows for these dynamics to be monitored in real time. The direction of the SPV shift is determined by the band bending at the interface (as the photoemission signals shift to higher or lower BEs in the case of surface depletion or accumulation, respectively). Of crucial importance to the work described here, XPS also enables chemically specific dynamics to be measured, i.e., the SPV shifts within the substrate and QD layer can be differentiated by monitoring different core level photoemission lines, giving a diagnostic of charge transfer between the QD and the substrate.[15]

Laser-pump X-ray-photoelectron-probe spectroscopy was performed at the TEMPO beamline at Synchrotron SOLEIL, the details of which are reported elsewhere.[15] Briefly, a continuous wave (CW) laser is used for photoexcitation, modulated

[a)]ben.spencer@manchester.ac.uk.
[b)]Present address: Department of Physics, King's College London, Strand, London WC2R 2LS, United Kingdom.

with a 50% duty cycle at a period $T = 1$–2 ms, during which fast XPS spectra are captured every 50 ns as the photoexcitation laser is turned on and off. Fast XPS is achieved using a delay-line detector with a resolution of 5 ns. The overall time resolution is 150 ns due to the spread of photoelectrons in the electron energy analyser and the speed of the electronics. This form of SPV spectroscopy has been implemented in order to study cases where the electron dynamics are intrinsically slow, for example, due to persistent photoconductivity (PPC) as at the ZnO $(10\bar{1}0)$ surface.[1,16,17] Two CW photoexcitation wavelengths, $\lambda = 372$ nm ($h\nu = 3.33$ eV, CUBE, Coherent) and 640 nm ($h\nu = 1.94$ eV, OBIS, Coherent), were chosen for photoexcitation of ZnO and PbS QDs, respectively; $h\nu = 1.94$ eV is insufficient to directly photoexcite the wide band gap oxide ($E_g \sim 3.3$ eV).

The earthed ZnO $(10\bar{1}0)$ surface (PI-KEM Ltd.) was prepared in ultra-high vacuum using Ar^+ sputtering and vacuum annealing cycles, as well as an anneal in 1–2×10^{-7} mbar O_2 as detailed previously.[17] The surface was diagnosed clean using XPS (absence of the C 1*s* photoelectron peak). The preparation and characterization of the colloidal PbS QDs has also been detailed elsewhere.[3] The QDs were surface passivated by cation exchange with Cd, and oleylamine ligands were exchanged with 3-mercaptopropionic acid (3-MPA) for chemically linking to the ZnO surface.[18] These QDs have recently been integrated into a solar cell that exhibited a power conversion efficiency of 6%, after further passivation using bifunctional organic ligands and halide anions.[3] Depth-profiling XPS and transmission electron microscopy (TEM) (see supplementary material)[19] were used to determine the PbS core diameter to be 3 ± 0.1 nm, with an effective band gap of 1.34 eV,[3] and a CdS surface "decoration" of effective thickness 0.15 ± 0.02 nm (i.e., a conformal CdS shell is not formed). The QDs were deposited onto the ZnO surface during a brief (1–2 min.) removal of the substrate from the vacuum chamber, and excess unbound QDs were washed away with solvent. The Langmuir isotherm effect together with the strong binding of the 3-MPA ligand to the ZnO surface ensured minimal adventitious contaminant adsorption during this process.[20] XPS was used to quantify how much carbon was associated with the 3-MPA ligands (containing S) and residual oleylamine ligands (containing N). 3-MPA accounted for 90% of the total ligands present, giving an expected ratio of N:S:C atoms of 1:9:45. The measured ratio was 1 ± 0.2:9.3 ± 1.9:40.1 ± 8.0, meaning that, within the limits of accuracy of the technique, the carbon signal was entirely associated with the organic ligands present, and not contaminants.[19] XPS photon energies were chosen to optimise surface sensitivity, with associated sampling depths (taken as three times the photoelectron inelastic mean free pathlength) of 1.6–1.9 nm, so an effective layer thickness of less than one QD is probed.[19] It is a necessary condition of the experiment that the Zn 3*d* signal is not obscured and the dosing conditions were adjusted to achieve this. Thus the experiment probes a dilute layer of QDs directly bound to the ZnO surface.

Fast XPS of the Zn 3*d* core level, with a photon energy of $h\nu = 175$ eV, was used to monitor the SPV at the ZnO surface. The QD layer was monitored via the Pb 4*f* core level using a photon energy of $h\nu = 280$ eV. Core level binding energies were extracted from the fitting of sum-approximation Voigt doublets with a Gaussian:Lorentzian mixing ratio of 70%.[21] The synchrotron radiation (SR) X-ray beam was measured to have a profile of 100 μm horizontally by 150 μm vertically. The laser photoexcitation beams had radii >5 times larger than the SR beam, allowing for a uniform excitation profile across the SR probe beam, with power densities of 0.22 and 0.16 W cm^{-2} for the $\lambda = 372$ and 640 nm lasers, respectively. Beam sizes at the sample position were measured using a photodiode translated in two dimensions, which was also used to spatially overlap the laser and SR beams.[15]

For an *n*-type semiconductor, the presence of surface states can give rise to upward band bending and the presence of a depletion layer at the surface. Upon illumination, the equilibrium band bending, V_0, is reduced as electrons are promoted into the conduction band (CB). Electrons migrate away from the surface as holes migrate towards the surface, reducing the surface field. The total change in the band bending, or SPV shift, ΔV_{SP}^{tot}, is described by[22]

$$\frac{\Delta V_{SP}^{tot}}{kT}\exp\left(\frac{\Delta V_{SP}^{tot}}{kT}\right) = \frac{n_P}{n_0}\exp\left(\frac{V_0}{kT}\right), \tag{1}$$

where n_P and n_0 are the photoexcited and doping carrier concentration respectively.

Figs. 1(a) and 1(b) show the transient SPV observed upon photoexcitation of the clean ZnO $(10\bar{1}0)$ surface. No SPV is observed using red (640 nm) photoexcitation, as expected, since the photon energy (1.94 eV) is considerably less than the band gap energy. With blue ($\lambda = 372$ nm) photoexcitation, a SPV shift of 90 meV is observed, as electrons are promoted across the ZnO band gap. It is immediately clear that the decay of the SPV in Fig. 1(b) occurs on slow timescales of the order of tens of microseconds. We associate this with the well-established PPC in ZnO,[1,16] which is primarily controlled by trapping at band gap states associated with ionized oxygen vacancy states resonant with the conduction band minimum (CBM).[17,23] Consistent with this, we find that a single or bi-exponential decay does not adequately fit the data. Instead, in Fig. 1, we model the decay of a SPV shift over time after photoexcitation using a stretched exponential[24]

$$\Delta V_{SP} = \Delta V_{SP}^{tot}\exp[-(t/\tau_\infty)^\beta], \quad 0 < \beta < 1, \tag{2}$$

where τ_∞ is the dark carrier lifetime. This model has been applied to a wide range of slow relaxation phenomena, including PPC caused by deep level traps in oxides and semiconductors,[25–27] as is proposed in ZnO $(10\bar{1}0)$.[17] β is a parameter that reflects the dynamic change in carrier lifetime as recombination occurs in materials with a distribution of recombination paths.[28] The onset of the SPV is correspondingly fitted according to[24]

$$\Delta V_{SP} = \Delta V_{SP}^{tot}(1 - \exp[-\alpha t]). \tag{3}$$

This reflects the competition between carrier generation and recombination. α therefore depends upon the photoexcitation fluence as well as the recombination rate.

Figs. 1(c) and 1(d) show the effects on the Zn 3*d* BE of photoexcitation with red and blue laser wavelengths when PbS QDs are chemically linked to the ZnO surface. In

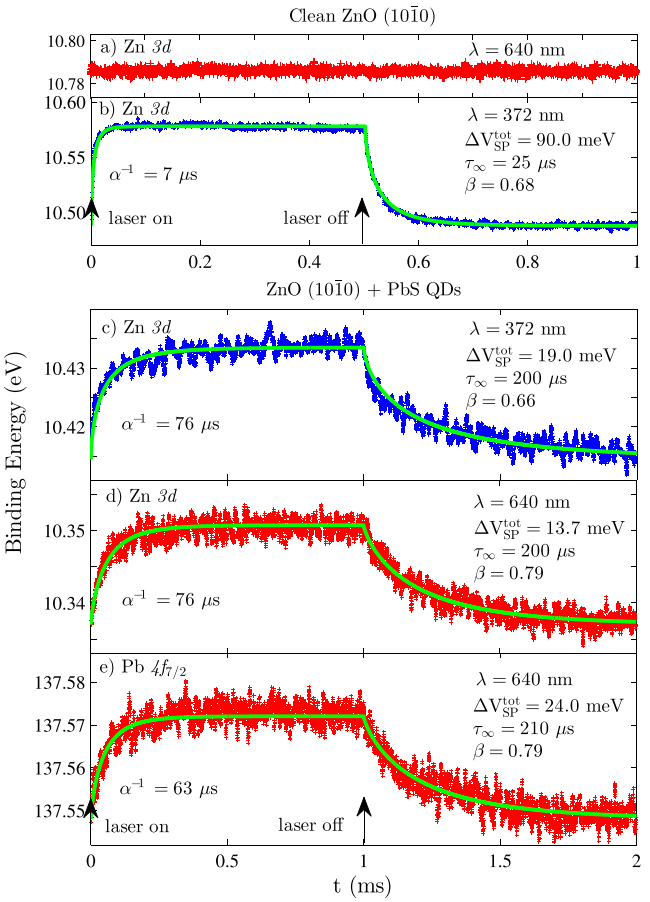

FIG. 1. Time-resolved binding energy (BE) shift of the Zn 3*d* core level at the clean ZnO (10$\bar{1}$0) surface before (a), (b), and after (c), (d) PbS QDs have been chemically linked using 3-MPA ligands, under illumination with $\lambda = 372$ nm (b), (c), and $\lambda = 640$ nm (a), (d) radiation. The time-resolved BE shift of the Pb $4f_{7/2}$ level of the QDs under illumination with $\lambda = 640$ nm radiation is shown in (e). The lasers are modulated at 50% duty cycle over a period of 1 (a), (b) and 2 (c)–(e) ms for the clean and QD-linked surfaces, respectively, as denoted by arrows. The decay and onset of the pump-induced surface photovoltage (SPV) (b)–(e) are fitted using stretched exponential decays and onsets (Eqs. (2) and (3), green lines); fitted parameters are listed (the total SPV shift, ΔV_{SP}^{tot}, dark carrier lifetime, τ_∞, decay exponent, β, and analogous onset constant, α^{-1}). (b)–(e) Data from the same surface.[19]

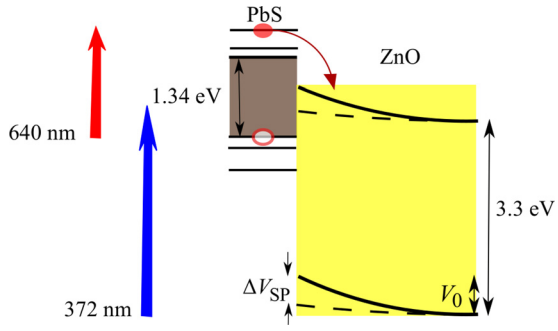

FIG. 2. Band alignment diagram for PbS quantum dots (QDs) chemically linked to the ZnO (10$\bar{1}$0) surface. Laser radiation with wavelengths of 372 and 640 nm are used for photoexcitation of the ZnO substrate and PbS QDs respectively. Photoexcitation of the QDs with 640 nm radiation allows for charge injection into the ZnO conduction band, which leads to a change in the equilibrium band bending, V_0, at the surface (the surface photovoltage shift, ΔV_{SP}). The diagram is constructed using the measured valence band alignment,[19] and the calculated effective band gap for 3 nm diameter PbS QDs.[3]

marked contrast to the result from the clean surface (Fig. 1(a)), a SPV onset and decay is now observed in ZnO under red illumination, which cannot directly photoexcite this surface. However, the red photon energy is sufficient to photoexcite the PbS QDs and is sufficient for electrons in the highest occupied molecular orbital (HOMO) in the PbS QD to be promoted to energies in excess of the ZnO CBM, as shown in Fig. 2. The observation of an induced SPV at the ZnO surface in this case is direct evidence of charge injection from the QDs into the ZnO surface.

The carrier lifetimes observed are now much longer than for the clean surface, both with fitted τ_∞ values of 200 μs. This is due to a reduced equilibrium band bending, V_0, caused by additional surface states at the QD-ZnO interface upon QD deposition; a reduced V_0 leads to a reduced total SPV shift (Eq. (1)) which in turn corresponds to extended carrier lifetimes.[17] We note that the decay of the PPC occurs over identical timescales for both blue and red photoexcitation. This indicates that the carrier lifetime after creation of carriers within ZnO, or after charge injection from the QDs into ZnO, is purely limited by the PPC in ZnO. The total SPV shift is less upon red illumination than for blue, 13.7 compared to 19 meV, due to the differences in fluence and absorption coefficient (hence n_P in Eq. (1)).

The use of XPS allows for differentiation of the charge dynamics of the substrate and the QDs. Fig. 1(e) shows the SPV shift of the Pb $4f_{7/2}$ level of the QDs bound to the ZnO surface under red illumination using identical conditions to Fig. 1(d). A SPV shift to higher binding energy of $\Delta V_{SP}^{tot} = 24$ meV is observed, with a dark carrier lifetime of $\tau_\infty = 210$ μs, identical within error to that observed in ZnO (Fig. 1(d)). The SPV shift is in the same direction as the Zn 3*d* core level (to higher binding energy) and indicates electron depletion.

The depletion layer width, w, is dependent on the dielectric constant of the material, ϵ_r, the doping concentration, and the equilibrium band bending[29]

$$w = \sqrt{2\epsilon_0\epsilon_r V_0/(n_0 e)}, \tag{4}$$

where ϵ_0 is the vacuum permittivity and e the electron charge. The carrier concentration in the ZnO surfaces is determined by the oxygen vacancy concentration ($1–6 \times 10^{17}$ cm^{-3} for the surfaces used here).[17,30] This implies depletion layer widths of 7–40 nm at the ZnO surface (obtained from a range of V_0 values,[17] and $\epsilon_r = 7.4$).[31] In a similar way, for a heterojunction which has a thick layer of PbS QDs at the interface with ZnO, we can estimate a depletion layer width in the range 60–300 nm, which agrees well with literature values (60–200 nm).[11–13,32] This estimate indicates that the PbS QDs in an operating heterojunction are subject to a depletion field that extends over distances much greater than both the effective QD layer thickness and the XPS sampling depths in our experiment. Our experiment reveals that the PbS QDs directly bound at the interface with ZnO lie within the depletion field extending from the ZnO surface. The similarities in both the direction of the SPV shift and the dynamics between the Pb and Zn SPV measurements indicate that the energy levels of the QDs are pinned to those of the ZnO substrate, as has been noted previously for PbS and PbSe.[5,7] The reported doping

densities for PbS QD layers ($1–4 \times 10^{16}\,cm^{-3}$),[11,12] suggest that $n_0^{QD} < n_0^{ZnO}$, and hence V_0 across the QD layer is greater than in ZnO, evidenced here by the larger total SPV shift of the Pb $4f_{7/2}$ level (Fig. 1(e)).

The β-parameter (Eq. (2)) reflects the number of pathways for recombination in a slowly relaxing system,[27] tending to unity for a single pathway.[24] It has thus been observed to depend upon temperature, and here we observe that the fitted values are dependent on laser wavelength (Fig. 1), with a constant value (0.79) for red illumination and a smaller constant value (0.66–0.68) for blue photons. This reflects an increase in the number of recombination paths under blue illumination, as the blue laser is sufficiently energetic to directly populate both the ZnO conduction band and the ionized oxygen vacancy states associated with PPC.[17,23]

Time-resolved SPV spectroscopy is a powerful tool for probing the carrier dynamics at interfaces. In the case of PbS QDs chemically linked to the ZnO $(10\bar{1}0)$ surface, illumination with photon energies resonant with and below the ZnO band gap energy has allowed for the injection of carriers from the PbS QD to the ZnO CB to be demonstrated. Upon injection into the substrate, the carrier dynamics are limited by the PPC in ZnO.[17,23] Whilst QDs allow for engineered band gaps that can absorb the majority of the solar spectrum, oxides such as ZnO that exhibit controllable PPC may be highly suited as photoanode materials, as recombination rates may be tuned by controlling the oxygen vacancy concentration to allow for efficient carrier extraction. An observed SPV shift in the QDs, which decays on similar timescales to the ZnO substrate, confirms that the depletion field at the heterojunction extends into the QD layer.[8,11–13,32] The laser-SR SPV technique offers a chemically specific diagnostic of charge injection and charge dynamics in heterojunctions that paves the way for further studies to clarify how these phenomena influence photovoltaic performance.

The research leading to these results received funding from the European Community's Seventh Framework Programme (FP7/2007-2013) under Grant Agreement No. 226716, allowing access to Synchrotron SOLEIL. Work was also supported by EPSRC (UK) under Grant No. EP/K008544/1. The data associated with this paper are openly available from The University of Manchester eScholar Data Repository: http://dx.doi.org/10.15127/1.297390.

[1]P. D. C. King and T. D. Veal, J. Phys.: Condens. Matter **23**, 334214 (2011).
[2]M. C. Beard, J. M. Luther, and A. J. Nozik, Nat. Nanotechnol. **9**, 951 (2014).
[3]D. C. Neo, C. Cheng, S. D. Stranks, S. M. Fairclough, J. S. Kim, A. I. Kirkland, J. M. Smith, H. J. Snaith, H. E. Assender, and A. A. Watt, Chem. Mater. **26**, 4004 (2014).
[4]J. Tang, K. W. Kemp, S. Hoogland, K. S. Jeong, H. Liu, L. Levina, M. Furukawa, X. Wang, R. Debnath, D. Cha, K. W. Chou, A. Fischer, A. Amassian, J. B. Asbury, and E. H. Sargent, Nat. Mater. **10**, 765–771 (2011).
[5]B. A. Timp and X.-Y. Zhu, Surf. Sci. **604**, 1335 (2010).
[6]C.-H. M. Chuang, P. R. Brown, V. Bulović, and M. G. Bawendi, Nat. Mater. **13**, 796 (2014).
[7]S. J. Hardman, D. M. Graham, S. K. Stubbs, B. F. Spencer, E. A. Seddon, H.-T. Fung, S. Gardonio, F. Sirotti, M. G. Silly, J. Akhtar, P. O'Brien, D. J. Binks, and W. R. Flavell, Phys. Chem. Chem. Phys. **13**, 20275 (2011).
[8]A. G. Pattantyus-Abraham, I. J. Kramer, A. R. Barkhouse, X. Wang, G. Konstantatos, R. Debnath, L. Levina, I. Raabe, M. K. Nazeeruddin, M. Grätzel, and E. H. Sargent, ACS Nano **4**, 3374 (2010).
[9]See http://www.nrel.gov/ncpv/images/efficiency_chart.jpg for "Highest confirmed conversion efficiencies for research cells," National Renewable Energy Laboratory, Golden, CO (accessed February 01, 2016).
[10]A. J. Labelle, S. M. Thon, S. Masala, M. M. Adachi, H. Dong, M. Farahani, A. H. Ip, A. Fratalocchi, and E. H. Sargent, Nano Lett. **15**, 1101 (2015).
[11]S. M. Willis, C. Cheng, H. E. Assender, and A. A. R. Watt, Nano Lett. **12**, 1522 (2012).
[12]P. R. Brown, R. R. Lunt, N. Zhao, T. P. Osedach, D. D. Wanger, L.-Y. Chang, M. G. Bawendi, and V. Bulović, Nano Lett. **11**, 2955 (2011).
[13]L.-Y. Chang, R. R. Lunt, P. R. Brown, V. Bulović, and M. G. Bawendi, Nano Lett. **13**, 994 (2013).
[14]L. Kronik and Y. Shapira, Surf. Sci. Rep. **37**, 1 (1999).
[15]B. F. Spencer, M. J. Cliffe, D. M. Graham, S. J. Hardman, E. A. Seddon, K. L. Syres, A. G. Thomas, F. Sirotti, M. G. Silly, J. Akhtar, P. O'Brien, S. M. Fairclough, J. M. Smith, S. Chattopadhyay, and W. R. Flavell, Surf. Sci. **641**, 320 (2015).
[16]C. F. Klingshirn, A. Waag, A. Hoffmann, and J. Geurts, *Zinc Oxide: From Fundamental Properties Towards Novel Applications* (Springer-Verlag, Berlin, Heidelberg, Germany, 2010).
[17]B. F. Spencer, D. M. Graham, S. J. O. Hardman, E. A. Seddon, M. J. Cliffe, K. L. Syres, A. G. Thomas, S. K. Stubbs, F. Sirotti, M. G. Silly, P. F. Kirkham, A. R. Kumarasinghe, G. J. Hirst, A. J. Moss, S. F. Hill, D. A. Shaw, S. Chattopadhyay, and W. R. Flavell, Phys. Rev. B **88**, 195301 (2013).
[18]B. F. Spencer, M. J. Cliffe, D. M. Graham, S. J. O. Hardman, E. A. Seddon, K. L. Syres, A. G. Thomas, F. Sirotti, M. G. Silly, J. Akhtar, P. O'Brien, S. M. Fairclough, J. M. Smith, S. Chattopadhyay, and W. R. Flavell, Faraday Discuss. **171**, 275 (2014).
[19]See supplementary material at http://dx.doi.org/10.1063/1.4943077 for details of the materials characterization.
[20]D. C. Grinter, T. Woolcot, C.-L. Pang, and G. Thornton, J. Phys. Chem. Lett. **5**, 4265 (2014).
[21]R. Hesse, P. Streubel, and R. Szargan, Surf. Interface Anal. **39**, 381 (2007).
[22]J. P. Long and V. M. Bermudez, Phys. Rev. B **66**, 121308 (2002).
[23]S. Lany and A. Zunger, Phys. Rev. B **72**, 035215 (2005).
[24]R. G. Palmer, D. L. Stein, E. Abrahams, and P. W. Anderson, Phys. Rev. Lett. **53**, 958 (1984).
[25]J. Z. Li, J. Y. Lin, H. X. Jiang, A. Salvador, A. Botchkarev, and H. Morkoc, Appl. Phys. Lett. **69**, 1474 (1996).
[26]A. Dissanayake, M. Elahi, H. X. Jiang, and J. Y. Lin, Phys. Rev. B **45**, 13996 (1992).
[27]E. R. Viana, J. C. González, G. M. Ribeiro, and A. G. de Oliveira, J. Phys. Chem. C **117**, 7844 (2013).
[28]L. H. Chu, Y. F. Chen, D. C. Chang, and C. Y. Chang, J. Phys.: Condens. Matter **7**, 4525 (1995).
[29]P. A. Cox, *The Electronic Structure and Chemistry of Solids* (Oxford University Press, New York, USA, 1987).
[30]W. Göpel, Surf. Sci. **62**, 165 (1977).
[31]H. Yoshikawa and S. Adachi, Jpn. J. Appl. Phys., Part 1 **36**, 6237 (1997).
[32]D. D. W. Grinolds, P. R. Brown, D. K. Harris, V. Bulovic, and M. G. Bawendi, Nano Lett. **15**, 21 (2015).